Study on the Static Characteristics of a Hybrid Stepping Motor by Combining Magnetic Circuit Method and Numerical Magnetic Field Analysis

Yiping Dou*, Youguang Guo**, Jianguo Zhu**, and Zhongwei Jiang***
* Faculty of Electric Engineering and Automation, Nanjing Normal University, Nanjing, 210042, China
** Faculty of Engineering, University of Technology, Sydney, P.O. Box 123, 1 Broadway, NSW 2007, Australia
*** College of Automation, Nanjing University of Aeronautics and Astronautics, Nanjing, 210016, China

***Abstract*--This paper reports the study on the static characteristics of a hybrid stepping motor by a hybrid method which combines the magnetic circuit and numerical field analysis. Key parts, including the air gap, teeth and slots, are modeled by a tooth layer unit (TLU) based on a series of magnetic field finite element solutions. The TLU is implemented with the other magnetic parts to form a complete magnetic circuit for calculation of the motor characteristics, providing good computational accuracy with short CPU time. Theoretical calculations are validated by experiments on a hybrid stepping motor prototype.**

***Index Terms*--Hybrid stepping motor, magnetic circuit and field analysis, static characteristic, tooth layer unit.**

I. Introduction

Stepping motors have been developed in response to the demand for a device capable of producing a definite angular displacement in a driven shaft and holding its position against a torque applied to the driven shaft. The most important performance of a stepping motor is the static characteristics, e.g. the relationship between the static torque and the tooth position angle of the stator and rotor. The development of an appropriate method for effective and accurate computation of the static characteristics would be very beneficial to the design and analysis of the stepping motor.

Among various types of stepping motors, the hybrid stepping motor (HSM) is the most commonly used in industry due to the advantages of high torque and high resolution [1]. A typical HSM comprises two axial halves, each of which is similar to a variable reluctance stepping motor with double-salient structure on the stator and rotor with many teeth. Between the two halves of the rotor is an axially magnetized permanent magnet (PM). The magnetic field distribution in such a structure is quite complex, and hence three-dimensional (3D) numerical field analysis by for example finite element analysis (FEA) is required for accurately calculating the motor parameters and performance [2].

Magnetic field FEA can take into account the details of the motor, such as the structure, dimensions, and non-linearity of magnetic properties of materials, but the computational time may be very long, especially for the machines with complex structures and 3D fluxes. On the other hand, the conventional magnetic circuit method needs much less CPU time, but the results may not be accurate enough. Therefore, it can be an effective approach to combine the magnetic circuit method and the magnetic field FEA, providing a flexibility of satisfactory computational accuracy and time.

In this paper, the static characteristics of a hybrid stepping motor (HSM) are investigated by a hybrid method combining the advantages of the magnetic circuit and numerical field analysis, providing satisfactory computational accuracy with short computational time. The theoretical calculation is validated by the experiments on an HSM prototype.

The magnetic circuit of HSM is established in combination with a key calculation model, the tooth layer unit (TLU) [3, 4]. The engineering rationality of TLU is analyzed by the FEA of magnetic field. The TLU and other magnetic parts of the HSM form a complete magnetic circuit, by which internal electromagnetic relationships can be worked out with higher accuracy than that by the pure magnetic circuit method. Meanwhile, the relationships between the motor characteristics and structural parameters can be quickly worked out through this magnetic circuit, which is quite beneficial for the design and analysis of the HSM. This method is also effective for motor optimization, which often requires a large number of iterations.

II. HSM Prototype

Fig. 1 illustrates the cutaway view of the HSM under study [4]. The rotor has 3 identical axial sections. Each of them consists of two halves with an axially magnetized PM of $AlNiCo_5$ in between. Table I lists the major structural parameters. In order to investigate the motor characteristics by the combined method of the magnetic circuit and field analysis, the TLU model should be firstly determined, as will described in Section III.

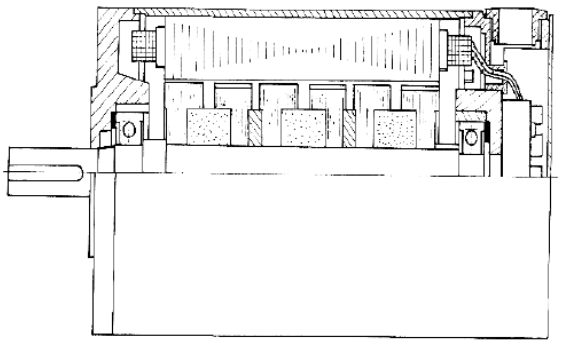

Fig. 1. Cutaway view of a hybrid stepping motor

TABLE I
MAJOR STRUCTURAL PARAMETERS OF AN HSM PROTOTYPE

Dimensions and parameters	Quantities
Number of stator poles	8
Number of teeth of each stator pole	5
Outside diameter of stator core (mm)	101.8
Inside diameter of stator core (mm)	59.4
Axial length of stator core (mm)	110.0
Number of rotor teeth	50
Number of rotor axial sections	3
Axial length of half the rotor section core (mm)	15.3
Number of permanent magnets	3
Outside diameter of magnet (mm)	42.0
Inside diameter of magnet (mm)	17.4
Axial length of each magnet (mm)	16.6
Number of turns of a phase winding	21

III. TLU CALCULATION MODEL AND RATIONALITY

A. TLU Rigion

Fig. 2 illustrates the TLU, which is a rectangular area with a width of a tooth pitch and is bordered by a line behind the stator tooth and a line behind the rotor tooth. TLU is the most complicated and important area for the distribution of magnetic field and the generation of torque. It is difficult to be dealt with by the magnetic circuit method, but becomes quite easy and accurate if the numerical field analysis is conducted. With FEA, the TLU model can fully take into account the non-linearity of the material and the non-uniform distribution of magnetic field in the teeth of stator and rotor.

Two assumptions are made for the TLU model: (a) Lines AB and CD are equipotential; (b) the fringing effect of the stator pole is ignored, i.e. all the stator teeth are assumed to have the same magnetic field distribution. These assumptions may cause computational errors, so the rationality of the model should be investigated to see if the computational accuracy can meet the requirement of engineering practice.

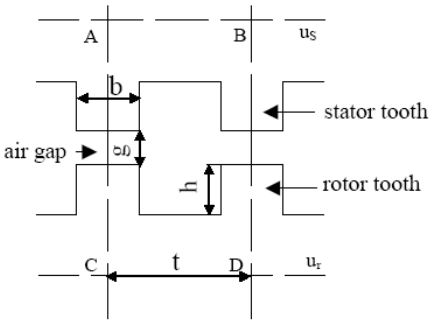

Fig. 2. The tooth layer unit

B. Rationality Analysis of TLU Model

1) Magnetic field FEA

When the fringing effect of axial end-surfaces is ignored, the magnetic field analysis can be carried out in a two-dimensional (2D) plane, e.g. a cross-sectional area of the HSM. Due to the structural symmetry, only half a pole pitch of the motor is required for the field solution, as shown in Fig. 3, where 1 is the current area, 2 stator core, and 3 rotor core. The surface arc effect of the iron core and the pole edge effect of the stator are considered in the calculation model, by which the magnetic potential values and their differences on the lines behind the teeth can be found out and the engineering rationality of the assumptions can be verified. There is only axial current in Fig. 3, and hence the Poisson's equation of magnetic potential vector A_Z is given by

$$\begin{cases} \dfrac{\partial}{\partial x}(\gamma\dfrac{\partial A_Z}{\partial x})+\dfrac{\partial}{\partial y}(\gamma\dfrac{\partial A_Z}{\partial y})=-J_Z, & \text{in area EFGHE} \\ A_Z=0, & \text{on broken line GHEF} \\ \gamma\dfrac{\partial A_Z}{\partial n}=0, & \text{on line FG} \end{cases} \tag{1}$$

where J_z is current density, γ reluctivity, and n the normal direction of line FG. After the magnetic vector potential $\boldsymbol{A}$ is solved, the magnetic flux density $\boldsymbol{B}$ and field strength $\boldsymbol{H}$ in each element can be determined by

$$\begin{aligned} B &= \nabla \times A \\ H &= \gamma B \end{aligned} \tag{2}$$

Fig. 3 shows the zero tooth position angle, where the most saturated state may happen in the motor. The magnetic field distributions with different currents, implying different saturation states, have been calculated. The magnetic force lines with a stator current density of 10 A/mm^2 (the rated density of the prototype is 8.6 A/mm^2), is illustrated in Fig. 4. The rationality of the basic assumptions will be analyzed through the magnetic equipotential lines, flux density and flux in the following sections.

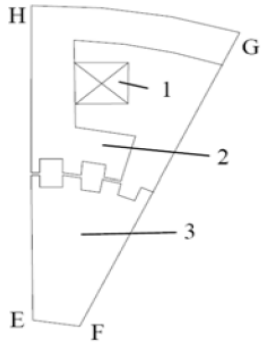

Fig. 3. Field solution region

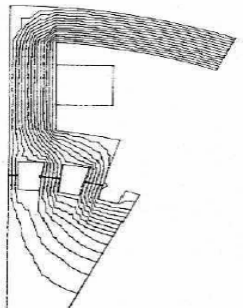

Fig. 4. Magnetic force lines produced by a stator current

2) Equipotential lines

The magnetic scalar potentials φ on the magnetic force lines at a radial height, h, can be calculated by

$$\varphi = \varphi_0 + \int_h H \cdot dh \tag{3}$$

The average is taken as the nominal value, φ_m, at a certain radial height If $\Delta\varphi_m$ is assumed as the maximum difference of φ on a scalar equipotential line and the relative error is given by $\varepsilon=\Delta\varphi_m/\varphi_m$, then the relative error ε on the line that is a tooth height far from the bottom of stator slot, is found to be less than 1.5%. Thus this line can be considered as equipotential. As to the line that is a tooth height far from the bottom of rotor slot, the same conclusion is obtained for the relative error ε is less than 1.0%.

3) Flux density

Fig. 5 shows two sample points (#1 and #2) in the middle tooth of stator pole and two points (#3 and #4) in the rotor tooth which faces the stator tooth, and four corresponding points (#1′, #2′, #3′, and #4′) in the outmost stator tooth and facing the rotor tooth. The flux densities at these points are calculated and analyzed to check the rationality of assumption (b).

Table II compares the flux densities at the sample point pairs under different stator currents (or current densities). The relative error is estimated by

$$\varepsilon = \frac{2|B_i - B_{i'}|}{B_i + B_{i'}} \times 100\%, \; i = 1, 2, 3, 4 \tag{4}$$

TABLE II
COMPARISON OF FLUX DENSITIES OF POINT-PAIRS

Point-pair number	J ($A \cdot mm^{-2}$)	2.5	8.0	10.0	20.0
1	B / T	0.768	1.414	1.466	1.722
	B′ / T	0.786	1.437	1.469	1.728
	ε / %	2.32	1.61	0.20	0.35
2	B / T	0.761	1.388	1.439	1.698
	B′ / T	0.766	1.375	1.432	1.682
	ε / %	0.65	0.94	0.49	0.95
3	B / T	0.732	1.325	1.375	1.624
	B′ / T	0.729	1.303	1.357	1.595
	ε / %	0.41	1.67	1.32	1.80
4	B / T	0.777	1.411	1.462	1.719
	B′ / T	0.774	1.375	1.430	1.670
	ε / %	0.39	2.58	2.21	2.89

The relative error between the magnetic flux density in the middle tooth and that in the edge is less than 3.0%. Thus, it can be considered that magnetic distribution in each tooth under the stator pole is approximately the same. The analysis region can thus be reduced to a tooth pitch area. That is to say assumption condition (b) of TLU is rational from the view of engineering calculation.

4) Flux

Based on assumption (b), the magnetic flux passing the stator pole is obtained by

$$\phi = Z_s \times \phi_0 \tag{5}$$

where ϕ is the flux of each pole, Z_s the tooth number of each pole, and ϕ_0 the flux of a TLU. Table III shows the calculations by (5) and that by numerical field analysis. The error is less than 3%, so the TLU can be used instead of the whole pole.

TABLE III
COMPARISON OF CALCULATED FLUX PER POLE

J ($A \cdot mm^{-2}$)	2.5	8.0	10.0	20.0
Flux by TLU (mWb)	0.0672	0.1208	0.1258	0.1489
Flux by whole pole (mWb)	0.0662	0.1183	0.1233	0.1456
ε (%)	1.51	2.11	2.03	2.27

So far, the calculation model of TLU has been studied by analyzing the magnetic scalar equipotential lines, flux density and flux. The results show that the calculation model can meet the accuracy requirement of engineering practice.

C. Determination of TLU

In Fig.1, the scalar potentials of the equipotential lines AB and CD are assumed as u_S and u_r, respectively, and the potential difference between the two lines is $F = u_s - u_r$. Lines AC and BD obey the periodical boundary conditions when the distribution of magnetic field is considered the same for every tooth pitch. The governing equation for solving the magnetic field in a TLU is given by

$$\begin{cases} \dfrac{\partial}{\partial x}(\mu \dfrac{\partial \varphi}{\partial x}) + \dfrac{\partial}{\partial y}(\mu \dfrac{\partial \varphi}{\partial y}) = 0 \\ \varphi|_{CD} = 0 \\ \varphi|_{AB} = F \\ \varphi(x, y)|_{AC} = \varphi(x + \lambda, y)|_{BD} \end{cases} \tag{6}$$

where φ is the scalar potential, μ the magnetic permeability, and λ the tooth pitch. For a given relative angle θ between the stator and rotor teeth and a magnetic potential difference F, the distribution of the magnetic field of TLU can be solved by 2D or 3D FEA. The magnetic parameters in each TLU, including the flux density B, field strength H, magnetic energy W_f, and specific magnetic conductance G, can then be determined. When the flux in a tooth pitch and per unit axial length of iron core, $\varphi(\theta, F)$ is obtained, the magnetic conductance can be calculated by

$$G = \varphi(\theta, F) / F \tag{7}$$

The amount of energy W_f per unit axial length is given by

$$W_f = \sum_{K_1+1}^{K_2} \int_0^{He} S_e B_e dH + \frac{1}{2} \sum_{1}^{K_1} \frac{S_e B_e^{\,2}}{\mu_0} \tag{8}$$

where e is the number of elements, B_e, H_e and S_e are the flux density, field strength, and area of element e, respectively, K_1 is the last number of the air elements, and K_2 is the total number of elements. Both G and W_f are related to the saturation of iron core and change with respect to the relative position angle θ and potential difference F.

IV. COMPLETE MAGNETIC CIRCUIT MODEL

The nonlinear magnetic circuit of HSM can be established by combining the magnetic conductance of the whole TLU and the other parts of HSM. The former is built based on the magnetic field FEA solutions and the latter is obtained by the classical magnetic circuit method based on circuit parameters. Considering the structural symmetry of magnetic circuit of the prototype, only half a pole pitch needs to be included in the complete magnetic circuit, as shown in Fig. 5, where the parameters are calculated as the following.

1) Magnetic conductance of TLU, G_{Fi} (i = 1, 2, 3, 4):

G_{Fi} is the function of θ and F for a known TLU and can be expressed as

$$G_{Fi} = Z_s lG(F, \theta + \frac{2\pi(i-1)}{m}) \tag{9}$$

where m is the number of phases, and l is the axial length of iron core.

2) Magnetic conductance of stator pole, G_{Fi} (i = 7, 8, 9, 10): Assume F_p is the magnetic scalar potential difference across the stator pole with an effective height h_p and a cross-section area A_p. The average magnetic field strength of the stator pole is then $H_p=F_p/h_p$. The flux density B_p can be obtained from the B-H curve of the pole material. Thus, the magnetic permeability $\mu_p=B_p/H_p$, and the conductance $G_{Fi} = \mu_p A_p/h_{p=}\Lambda(F_p)$.

3) PM conductance and Leakage conductance of the PM and those between the poles, G_{Fi} (i=5, 6, 11~16): These conductances are almost constant and can be calculated by $G_{Fi} = \mu_i A_i/h_i$, where μ_i is the magnetic permeability of air or magnets, A_i the cross-sectional area, and l_i is the length of the corresponding part of the magnetic circuit.

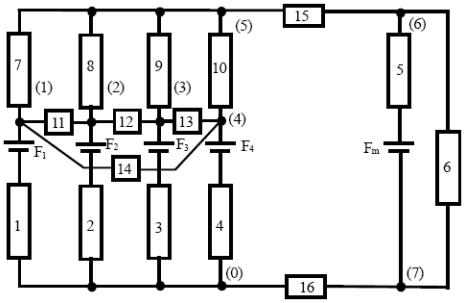

Fig. 5. Complete magnetic circuit of the HSM

4) Magnetomotive force (mmf): The *mmf* produced by the PM is $F_m=H_c l_m$, where H_c is the coercive force of PM, and l_m is the length along the magnetization direction. The *mmfs* produced by the stator currents are $F_i=NI_i$ (i=1, 2, 3, 4), where N is the number of turns of the coil of a pole, and I_i is the current of phase i.

By the nodal analysis method, the equation for solving the nodal potentials can be written in a matrix form: $[G_F] = [\vartheta]'[\Phi]'$, where $[G_F]$ is the conductance matrix, $[\vartheta]'$the array of the nodal magnetic potential, and $[\Phi]'$ the array of the equivalent magnetic flux. As G_F is a function of ϑ, the equation is nonlinear and can be solved by the iterative method.

V. Magnetic Energy and Static Torque

Given a tooth position angle θ and a potential difference F, the total energy of a TLU can be readily obtained from the specific magnetic energy W_f, already known by (8), by $W_{fi}=Z_s l W_f$. The magnetic energy in linear materials is $W_{fi}=\Phi_i^2/(2G_{Fi})$, where Φ_i and G_{Fi} are the flux and equivalent conductance of a linear part of the magnetic circuit. The magnetic energy in the pole is calculated based on the non-linear B-H curve of the pole material by

$$W_{fi} = V_i \int_0^H BdH \tag{10}$$

where V_i is the volume of the pole. The total magnetic energy of the motor, W_{ft} is the sum of the energies of all parts of the magnetic circuit.

The static torque T of the motor is a function of the stator current I and tooth position angle θ, and can be calculated by

$$T = \frac{\partial W_f}{\partial \theta}\Big|_{I=C} \approx \frac{\Delta W_f}{\Delta \theta}\Big|_{I=C} \tag{11}$$

Fig. 6 illustrates the static torque versus rotor position curve of the HSM prototype when the excitation current is 5 A, by using the combined method. To check the validity of the combined calculation procedure, the torque is also measured and plotted in Fig. 6. It can be seen that the calculations agree well with the measured results.

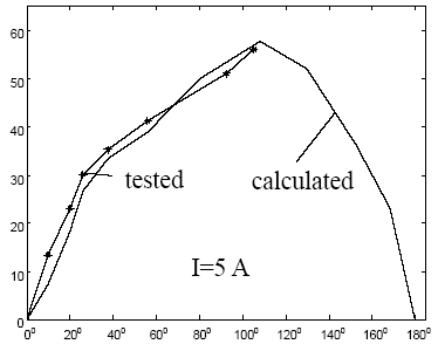

Fig. 6. Calculated and measured static torque of an HSM prototype

VI. Conclusion

The method presented in this paper has the advantages of both the conventional magnetic circuit method and advanced numerical field analysis, and hence can provide a good computational accuracy with a short CPU time. The theoretical calculations are verified by the experimental measurements on a hybrid stepping motor prototype. This combined method can also be used for design and analysis of other types of electromagnetic devices.

References

[1] K.C. Kim, J.P. Hong, and G.T. Kim, "Characteristics analysis of 5-phase hybrid stepping motor considering the saturation of both teeth and poles," in *Proc. IEEE Industry Applications Society Annual Meeting*, 2000, pp. 132-138.

[2] T. Kosaka, C. Pollock, and N. Matsui, "3 dimensional finite element analysis of hybrid stepping motors taking inter-lamination gap into account," in *Proc. IEE*, 2004, pp. 534-539.

[3] G.X. Han, Z.P. Wang, Z. Cheng, and S. Hirobumi, "A precise non-linear simulation model for hybrid stepping motor," in *Proc. the 5th Int. Conf. on Electrical Machines and Systems*, Aug. 2001, Shenyang, China, pp. 986 – 990.

[4] Y.P. Dou, "The engineering rationality of a hybrid stepping motor calculation model," in *Proc. the 8th Int. Conf. on Electrical Machines and Systems*, Sept. 2005, Nanjing, China, pp. 738-741.